International Journal of Fluid Machinery and Systems
Vol. 6, No. 4, October-December 2013

DOI: http://dx.doi.org/10.5293/IJFMS.2013.6.4.170
ISSN (Online): 1882-9554

Original Paper (Invited)

Effect of Axial Spacing between the Components on the Performance of a Counter Rotating Turbine

Rayapati Subbarao and Mukka Govardhan

Department of Mechanical Engineering, IIT Madras
Chennai, 600036, India, rsubbarao@hotmail.com, gova@iitm.ac.in

Abstract

Counter Rotating Turbine (CRT) is an axial turbine with a nozzle followed by a rotor and another rotor that rotates in the opposite direction of the first one. Axial spacing between blade rows plays major role in its performance. Present work involves computationally studying the performance and flow field of CRT with axial spacing of 10, 30 and 70% for different mass flow rates. The turbine components are modeled for all the three spacing. Velocity, pressure, entropy and Mach number distributions across turbine stage are analyzed. Effect of spacing on losses and performance in case of stage, Rotor1 and Rotor2 are elaborated. Results confirm that an optimum axial spacing between turbine components can be obtained for the improved performance of CRT.

Keywords: Counter Rotating Turbine, Axial Spacing, Turbine Performance, Pressure Coefficient.

1. Introduction

Increasing demand for the improvement of efficiency, reduction of weight and consideration of fuel consumption in case of aircraft engines lead the researchers to arrive at an unconventional turbine known as counter rotating turbine that has two rotors. Conventional axial flow turbine consists of stationary vanes (nozzles) and rotating blade rows (rotors) consequently placed in the flow path. In case of counter rotating turbines, nozzle will be followed by a rotor and then a second rotor that rotates in the opposite direction of the first one. It means that the blade rows are joined to two shafts with opposite direction of rotation. Such placement of flow path elements gives benefits, but needs special approach to organize flow inside the turbine. Special attention must be paid to the selection of optimal rotation speed and flow radial equilibrium conditions. Modern aerodynamic designs, computational and optimization methodologies allow us to fulfill this task in the shortest period of time with the highest gain in turbine performance. Other than the advantages mentioned earlier, it can reduce the torque on aircrafts that results in increasing maneuverability. Also, vane elimination in CRT helps in increasing the efficiency and decreasing the stage weight and axial length. Efficiency of a two-stage CRT was first analyzed in terms of work and speed requirements by Wintucky and Stewart [1]. It was assumed that the advantage aspect might be due to the removal of the inter-stage stator. Ozgur and Nathan [2] considered a particular counter rotating turbine stage with and without guide vanes that has axial inlet and outlet velocities, equal rotation speeds and specific work in each blade row. Louis [3] analyzed both the types of CRTs and found that stage loading coefficients were higher when compared with the conventional one. As far as the computational studies on counter rotating turbines are concerned, Ji et al. [4] of Chinese Academy of Sciences was the first to investigate about the work capability of vaneless CRT. Zhao et al. [5] found that using CRT with the same number of stages as in the prototype, it would be possible to obtain the same performance level, with decrement in turbine axial length by 30% and weight by eliminating vanes.

Studies have been made to investigate the effect of axial spacing on the aerodynamic performance of turbine stage, and some efforts among them revealed the importance of unsteadiness and the mechanism of losses in turbomachinery. Venable et al. [6] and Yamada et al. [7] studied the influence of axial spacing between the blade rows on the aerodynamic performance in a turbine stage and found increment of axial spacing to be advantageous. On the other hand, the experimental and numerical analysis of Jeong et al. [8] revealed decrement of efficiency with the increase in axial spacing in case of a supersonic impulse turbine. Also, Gaetani et al. [9] and Kikuchi et al. [10] reported that it was possible to achieve higher turbine efficiency with decreased axial spacing. Investigations on impulse turbine by Sadovnichiy et al. [11] discovered drop in efficiency when the axial spacing was increased for one configuration, but for another configuration the efficiency remained almost unchanged. Since the performance variation with respect to axial spacing is not clear from the literature, it is needed to conduct a study that would bring more information about the effect of this constraint. Also, the effect of axial spacing in case of CRT has not been studied yet. In this context, present

Received July 29 2012; revised January 21 2013; accepted for publication February 28 2013: Review conducted by Prof. Hyung-Hee Cho. (Paper number O13012S)
Corresponding author: Rayapati Subbarao, Scholar, rsubbarao@hotmail.com
This paper was presented at 5th International Symposium on Fluid Machinery and Fluids Engineering, October 24-27, 2012, Jeju, Korea.

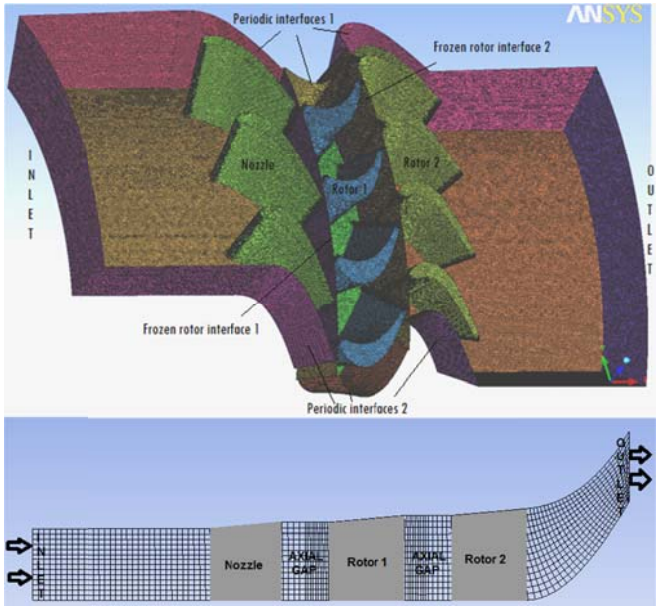

Fig. 1 Sectional and Meridional views of CRT domain.

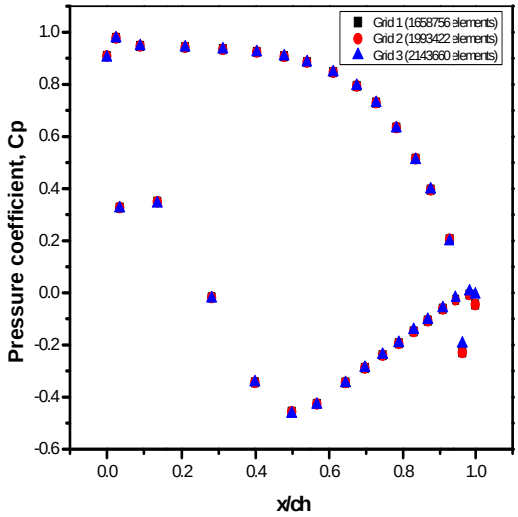

Fig. 2 Grid independence study.

work primarily aims at studying the effect of varying axial spacing on the performance and flow field of CRT. Mass flow rates of 3-7.5 kg/s per domain and axial spacing of 10, 30 and 70% are considered in the present investigation.

2. Methodology

Computational domain of CRT consists of Nozzle, Rotor 1 and Rotor 2 as shown in Fig.1. Modified details of the geometric configuration obtained from Dring et al. [12] are shown in Table 1. Tip clearance is considered for the rotor. Each axial spacing and stage requires modeling and grid generation of fluid domain consisting of all the components. Model is generated using the Cartesian coordinates for the hub, tip and blade. X-axis is chosen as the axis of revolution. Flow is treated as periodic and domain of the nozzle is taken with three blades and that of rotors is taken with four blades to reduce the computational time and cost substantially. For grid generation, tetra meshing is used. For improved mesh quality, it incorporates a powerful smoothening algorithm as well as tools for local adaptive mesh refinement and coarsening. For better modeling of near-wall physics of the flow field, prism meshing is done that consists of layers near the boundary surfaces and tetrahedral elements in the interior. Modeling and meshing of the computational domain are done using the commercial software ANSYS® ICEM CFD 13.0. Mesh distribution is done to provide sufficiently large number of elements in the tip clearance region, near the leading and trailing edges and around the blade. Nozzle, Rotor 1 and Rotor 2 consist of about 2.0, 2.0 and 2.5 million elements respectively. CFX 13.0 is used for simulations. Total pressure at nozzle inlet and mass flow rate at rotor 2 outlet are specified as boundary conditions. Flow parameters are as shown in Table 2. Inlet flow is assumed to be uniform with no swirl. Air ideal gas is considered as the working fluid. All surfaces viz. hub and tip end walls and the blade surfaces are given smooth wall with no-slip boundary condition. Rotational periodicity is enforced about the axis of rotation. Standard k-ω based Shear Stress Transport (SST) model is used as it accounts for the transport of turbulent shear stress and the amount of flow separation under adverse pressure gradients. In order to see that the results are not dependent on the grid size, grid independence study is carried out by changing the number of elements. Figure 2 shows the C_p distribution in case of nozzle for three grid sizes. It is observed that the results are not changing with the number of elements. Also, this study is helpful in selecting the grid size for further analysis.

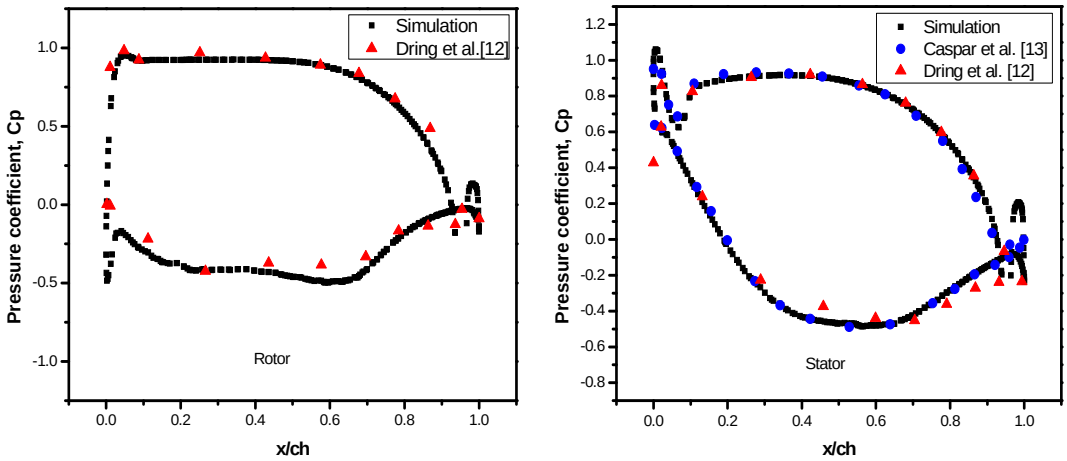

Fig. 3 C_p distribution of Rotor and Stator.

Table 1 Blade configuration used in CRT

Parameters	Nozzle	Rotor 1	Rotor 2
Number of airfoils	22	28	28
Hub radius (mm)	610	610	610
Tip radius (mm)	762-776	776-790	790-805
Tip clearance (mm)	0	2.28	2.28

Table 2 Flow parameters used in the simulation

Parameters	Values
Inlet temperature (K)	480
RPM of rotors	600
Inlet flow turbulence	1%
Mass flow rate per domain (kg/s)	3-7.5

3. Results Analysis

3.1 Validation

Simulation results are validated with the experiments conducted in a one and one-half stage large scale rotating turbine rig at the United Technologies Research Center (UTRC), USA. Pressure coefficient (C_p) distribution of rotor and stator are used for comparison with the experimental values of Dring et al. [12] as shown in Fig. 3. In case of rotor, flow accelerates smoothly from the leading edge to trailing edge on the pressure side. On the suction surface, there is a peak velocity near the leading edge followed by acceleration to the throat. From the throat, flow decelerates smoothly to the trailing edge without separation. The agreement is excellent except for a small region on the suction side where the simulation trough is visible at the leading edge. In case of stator, on the pressure side, there is distinct nature of flow near the leading edge because of rotor flow incidence. After that the velocity decreases till throat and then accelerates. On the suction surface, flow accelerates smoothly towards the mid-chord of the vane. From throat, flow decelerates smoothly to the trailing edge without separation. Simulation values are in agreement except for a small region on the pressure side where the peak amplitude is shifted to the left of the experimental one. Comparison is also made with the potential flow calculation presented by Caspar et al. [13]. Overall, the match between the simulation and experimentation is good in both rotor and stator cases.

3.2 Velocity distribution and flow around the vanes

Figure 4 describes the streamlines of velocity along the mid-span of the blade passage for x/ch = 30%. Flow along the blade passage at mid-span locations turns with the passage contour and effectively follows ideal behaviour. At zero degree angle of incidence, the streamline splits at the stagnation corresponding to the blade leading edge with one patch moving along the pressure side and the other moving along the suction side of the blade. Pressure gradient from one side to another side of the vane leads to development of secondary flows. In case of nozzle, on the pressure side, velocity increases steadily from leading edge to the trailing edge because of the reduction in pressure. Along the suction surface, velocity initially increases towards the throat, starts decreasing downstream of the throat. The peak velocity corresponds to the location of the minimum C_p on the suction surface, as

the flow beyond this changes direction and follows the blade shape. In case of rotors, on the suction surface, velocity increases up to the throat and then decelerates towards the trailing edge. On the pressure surface, velocity decreases up to mid-chord and slowly increases towards end of the vane. Flow around Nozzle, Rotor 1 and Rotor 2 is clearly shown in the figure separately.

3.3 Static pressure, axial velocity and Mach number distributions

Figure 5 shows the static pressure distribution along with velocity vectors at the mid-chord of Rotor 1 and Rotor 2 for x/ch = 70%. Leakage of flow through the tip gap and tip clearance vortex is seen along with the velocity vectors. It is also observed that there is low pressure zone at the entry to the tip gap and at the core of the tip clearance vortex. Same pattern is observed in case of Rotor 2 as well. Figure 6 shows contours of axial velocity coefficient (normalized by tip velocity) at the exit of Rotor 1 and Rotor 2 for x/ch = 10%. From hub to tip, velocity coefficient values changed considerably in both the rotors. Velocity levels are high near the trailing edge than near the end wall. It is seen that the flow behavior is similar at the exit of rotors. Figure 7 shows the distribution of Mach number from hub to tip for rotor blade rows in case of 30% spacing. At rotor inlet, the Mach numbers are high near the hub than the tip. Mach number values increased at the leading edge regions of the vanes near the tip and decreased near the hub along the span towards the exit of the CRT stage. These axial velocity and Mach number distributions indicate the three-dimensionality and complex nature of the flow in CRT.

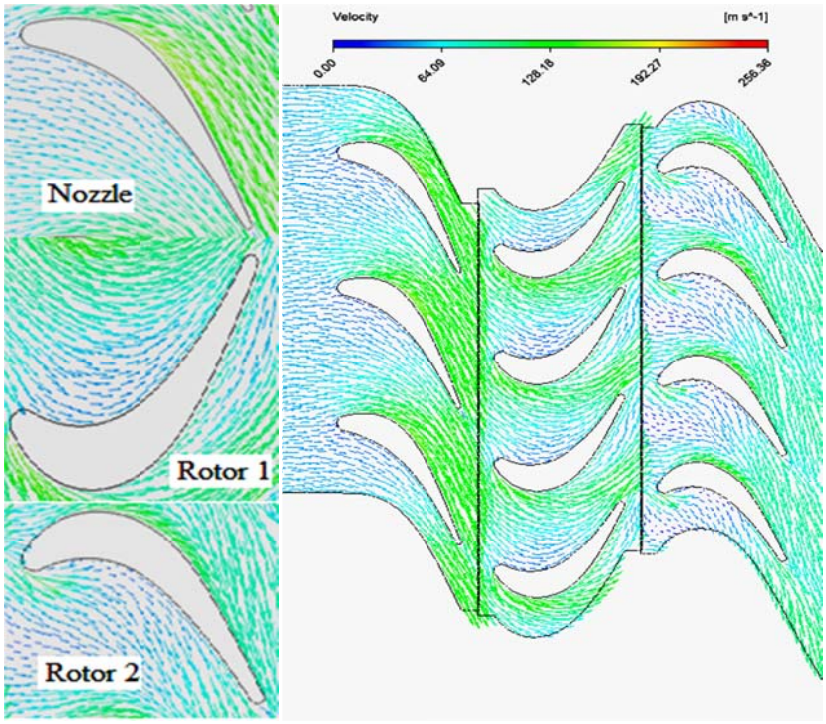

Fig. 4 Velocity streamlines and distribution across the stage for 30% spacing.

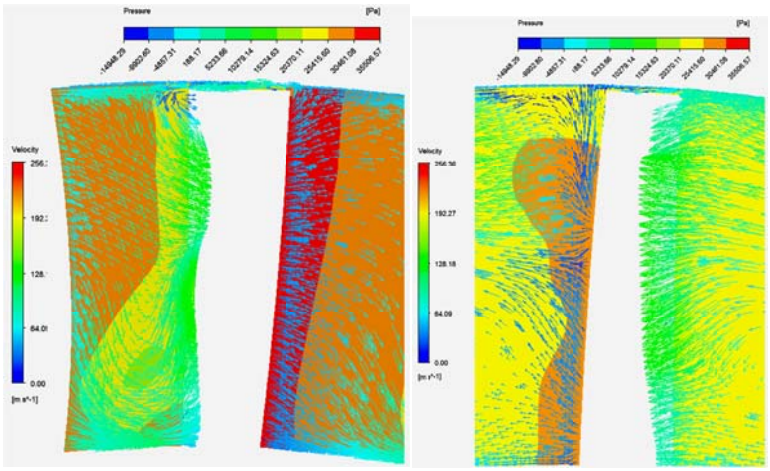

Fig. 5 Static pressure distribution with velocity vectors at the mid-chord of Rotor 1 and Rotor 2.

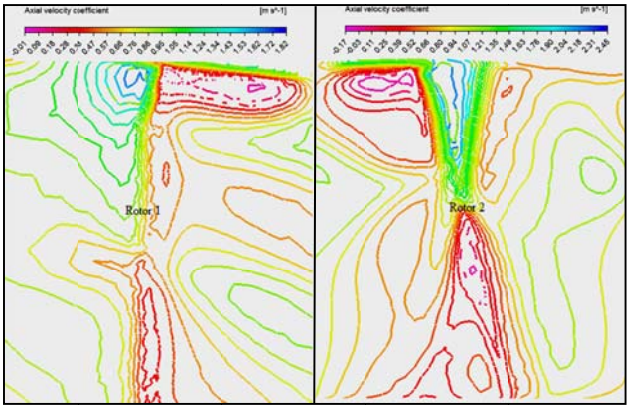

Fig. 6 Axial velocity coefficient at the exit of Rotor 1 and Rotor 2.

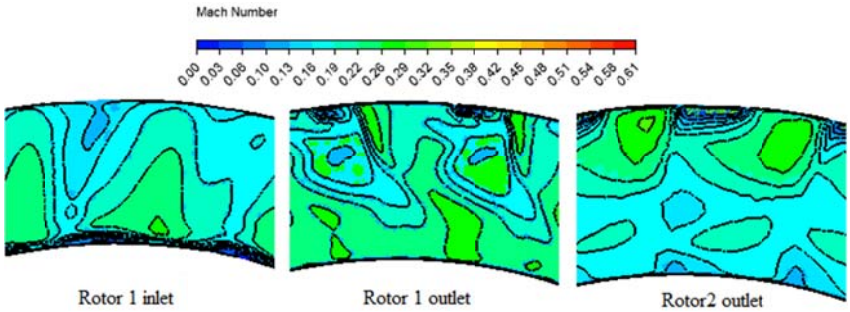

Fig. 7 Mach number distribution at various sections of CRT.

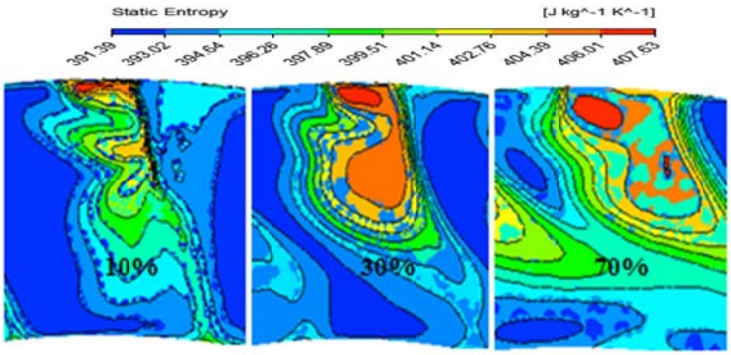

Fig. 8 Entropy at the exit of Rotor 1 with axial spacing.

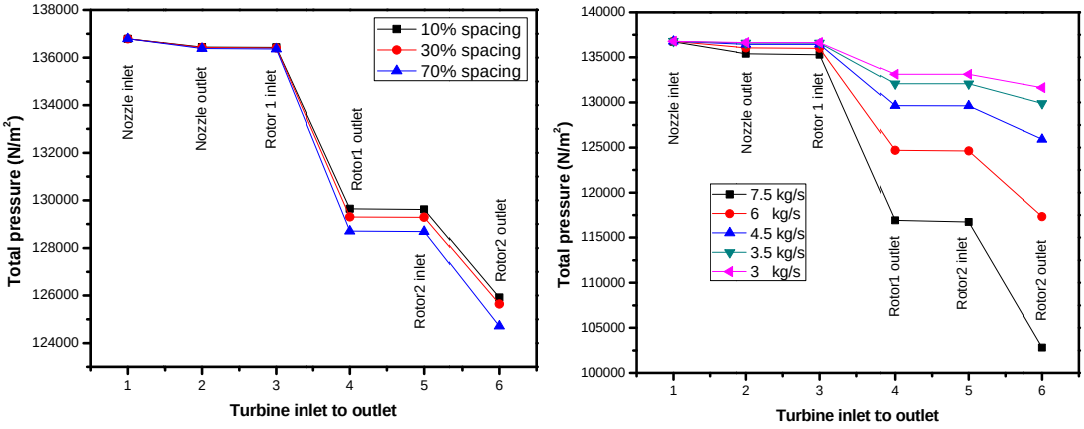

Fig. 9 Total pressure variation with axial spacing and mass flow rate.

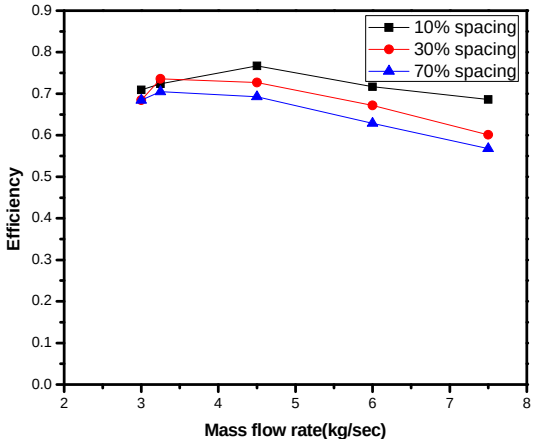

Fig. 10 Efficiency of CRT with mass flow rate.

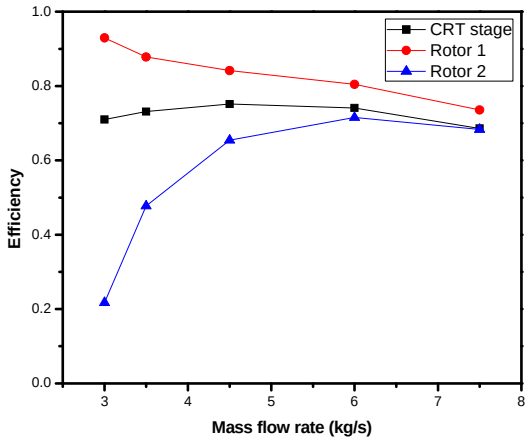

Fig. 11 Comparison of Rotor 1 and Rotor 2 with CRT stage.

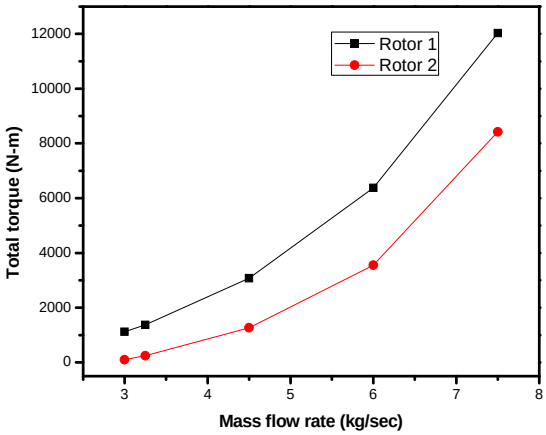

Fig. 12 Torque from rotors with flow rate.

3.4 Entropy and total pressure difference

Entropy values enable us to identify losses as well as wake generation regions. Figure 8 shows the entropy distribution at the exit plane of Rotor 1. The entropy generation inside the rotor is due to the rotational effects and due to non-uniform inlet flow from the nozzle. At x/ch = 10%, the entropy generation is less, but the strength of the wakes and vortices is more because of improper mixing at the interface. Interestingly, the loss core regions are more in case of lesser and higher spacing than the intermediate one (30%). The high loss region near the mid-passage is recognized in the form of wakes formed near rotor trailing edge. With respect to the spacing and mass flow rate, total pressure losses in the rotors vary significantly. Total pressure across the turbine stage with axial spacing and mass flow rate is shown in Fig. 9. Same outline of pressure variation is observed in all the spacing. But, the magnitude of difference in rotors varied. For the flow rate of 4.5 kg/s considered here, pressure change in Rotor 1 is increased as the spacing is increased. It is about 13% more when the spacing is changed from 10% to 70%. This is for the flow rate of 4.5 kg/s. In case of rotor 2, the total pressure difference increased the same way as in case of Rotor 1. It is about 7% more in case of the higher spacing compared with the lowest. Thus, spacing plays role in the amount of energy being converted by rotors in a turbine stage. With mass flow rate, the total pressure varied systematically, suggesting the deviation in the available energy for conversion in rotors. Pressure changes are more in case of higher flow rates.

3.5 Performance with mass flow rate and spacing

Figure 10 shows the variation of efficiency with mass flow rate. At lower mass flow rates, the efficiency does not vary much with the axial spacing. At mass flow rate of 4.5 kg/s, highest efficiency is obtained at 10% spacing. For the mass flow rate of 3.5 kg/s and less, 30% spacing is giving better performance. It is confirmed that axial spacing plays important role in deciding the highest performance point based on the flow condition. This aspect is not detailed till now in case of counter rotating turbine. Figure 11 shows the part played by Rotor 1 and Rotor 2 with respect to the overall stage for all the mass flow rates. The performance of Rotor 1 decreased with flow rate. Rotor 2 performance increased with flow rate and gets stabilized after a certain optimum value. Torque obtained from Rotor 1 and Rotor 2 is shown in Fig. 12. Both the rotors showed the same behaviour and torque obtained increased with flow rate. For lower mass flow rates, torque values changed slightly. At higher flow rates, torque values changed swiftly.

4. Conclusions

In this work, flow parameters like velocity, pressure and Mach number and performance parameters like torque and efficiency are studied. Flow along the blade passage at the mid-span locations effectively followed ideal behaviour. Axial velocity coefficient and Mach number contours showed the three dimensional and complex nature of the flow in CRT. As the spacing is increased, the total pressure variation in Rotor 1 increased more compared to Rotor 2. In case of rotor exit planes, from hub to tip, the losses increased gradually, indicating the presence of tip secondary flows. Effect of axial spacing on the flow structure around the vanes and the performance comparison of both the rotors is discussed here which is not dealt previously. Total pressure losses, torque obtained from rotors and efficiency varied with respect to spacing and mass flow rate. It is confirmed that the aerodynamic performance of CRT is dependent on axial spacing and can be optimized for a given configuration.

Nomenclature

Ch	Chord length [m]	x	Distance along x-axis [m]
CRT	Counter Rotating Turbine	ΔH	Enthalpy change
C_p	Pressure coefficient, $\frac{P-P_{static,out}}{P_{total,in}-P_{static,out}}$	$\dot{m}$	Mass flow rate (kg/s)
η	Efficiency, $\frac{Power\ output}{\dot{m} \times \Delta H}$		

References

[1] Wintucky, W.T., Stewart, W.L., 1957, "Analysis of two-stage counter-rotating turbine efficiencies in terms of work and speed requirements," NACA RM E57L05.

[2] Ozgur, C., Nathan, G.K., 1971, "Study of contra-rotating turbines based on design efficiency," Journal of Basic Engineering, Vol. 93, pp. 395-404.

[3] Louis, J.F., 1985, "Axial flow contra-rotating turbines", ASME paper, 85-GT-218.

[4] Ji, L.C., Quan, X.B., Wel, L., Xu, J.Z., 2001, "A Vaneless Counter rotating turbine design towards limit of specific work ratio," ISABE paper, 2001-1062.

[5] Zhao, Q.H., Du, J., Wang, H.S., Zhao, X.L., Xu, J.Z., 2010, "Tip clearance effects on inlet hot streak migration characteristics in high pressure stage of a vaneless counter-rotating turbine," Journal of Turbomachinery, Vol. 132, No. 011005, pp. 1-8.

[6] Venable, B.L., Delaney, R.A., Busby, J.A., Davis, R.L., Dorney, D.J., Dunn, M.G., Haldeman, C.W., Abhari, R.S., 1999, "Influence of vane-blade spacing on transonic turbine stage aerodynamics. Part I - time-averaged data and analysis," Journal of Turbomachinery, Vol. 121, pp. 663-672.

[7] Yamada, K., Funazaki, K., Kikuchi, M., Sato, H., 2009, "Influences of axial gap between blade rows on secondary flows and aerodynamic performance in a turbine stage," GT 2009-59855.

[8] Jeong, E., Park, P.K., Kang, S.H., Kim, J., 2006, "Effect of nozzle-rotor clearance on turbine performance," ASME paper, FEDSM 2006-98388.

[9] Gaetani, P., Persico, G., Dossena, V., Osnaghi, C., 2006, "Investigation of the flow field in a hp turbine stage for two stator-rotor axial gaps, Part I-3D time-averaged flow field," GT 2006-90553.

[10] Kikuchi, M., Funazaki, K., Yamada, K., Sato, H., 2008, "Detailed studies on aerodynamic performance and unsteady flow behaviors of a single turbine stage with variable rotor-Stator axial gap," International Journal of Gas Turbine, Propulsion and Power Systems, Vol. 2, No. 1, pp. 30-37.

[11] Sadovnichiy, V.N., Binner, M., Seume, J.R., 2009, "The influence of axial gaps and leaned-twisted guide vanes on the shroud leakage and turbine stage efficiency," Proceedings of the 8th European Conference on Turbomachinery, Austria.

[12] Dring, R.P., Joslyn, H.D., Blair, M.F., 1987, "The effect of inlet turbulence and rotor/stator interactions on the aerodynamics and heat transfer of large scale rotating turbine model," NASA CR-179469.

[13] Caspar J.R., Hobbs., D.E., Davis, R,L., 1980, "Calculation of two-dimensional potential cascade flow using finite area methods," AIAA Journal, Vol. 18, pp. 103-109.